European Polymer Journal 200 (2023) 112539

Contents lists available at ScienceDirect

European Polymer Journal

journal homepage: www.elsevier.com/locate/europolj

Synthesis, characterization, and optical properties of ROMP copolymers with pendant carbazole and coumarin groups

Mario Carratù [a], Rubina Troiano [a], Chiara Costabile [a], Antonella Caterina Boccia [b], Stefania Pragliola [a,*], Fabia Grisi [a,*]

[a] Dipartimento di Chimica e Biologia "Adolfo Zambelli", Università di Salerno, Via Giovanni Paolo II 132, I-84084 Fisciano, Salerno, Italy
[b] Istituto di Scienze e Tecnologie Chimiche "G. Natta" (SCITEC), Consiglio Nazionale delle Ricerche, Via A. Corti, 12, 20133 Milano, Italy

ARTICLE INFO

Keywords:
ROMP
Norbornene dicarboximide monomers
Carbazole
Coumarin
Fluorescent copolymers
Energy transfer

ABSTRACT

Two series of random copolymers containing at the same time two fluorescent groups, carbazole and coumarin, linked to a poly(norbornene dicarboximide) backbone have been prepared by controlled ring-opening metathesis polymerization (ROMP), promoted by Grubbs' third generation catalyst (**G3**). The relative amount of the two functionalities was systematically varied along the copolymer chain, and the high degree of structural control observed allowed also for the preparation of a block copolymer with an equimolar content of fluorophore groups.

In comparison to the related homopolymers, all the random copolymers exhibited in solution typical photoluminescence due to the carbazole or coumarin moiety, together with fluorescence arising from the energy transfer from the donor carbazole groups to the acceptor coumarin groups. This energy transfer seems to occur through intramolecular interactions, as it is not observed in the block copolymer and in the 50/50 homopolymer blend. On the other hand, in the solid state also the energy transfer from carbazole to coumarin through interchain interactions can take place. Of note, moving from solution to solid state fluorescence analysis, a blue shift of the band related to the energy transfer phenomenon is observed. This finding could be related to a combined effect of energy and electron transfer from donor to acceptor.

1. Introduction

Over the last decades, fluorescent molecules have received great scientific attention for their fascinating properties and important applications in various fields of materials and life science, including bioimaging, chemosensing and optoelectronic devices [1–7].

Fluorescent polymer materials have gained increasing interest because they show some advantages over small molecules materials, such as good processability, film-forming ability and thermal stability, as well as amplification of fluorescence signal and enhanced optical stability [8–11].

Fluorescent polymers can be prepared by different polymerization techniques, such as cationic/anionic/radical polymerization [12–17], Ziegler-Natta coordination polymerization [18–21] or ring opening metathesis polymerization (ROMP) [22–24]. ROMP, especially promoted by ruthenium-based catalysts, is widely recognized as a valuable synthetic methodology to fabricate nonconjugated polymers, since it offers several advantages, including operational simplicity, high tolerance towards a variety of functional groups and fast reaction rate [25–28]. Moreover, both molecular weight distribution and dispersity of polymers can be controlled [26,28].

Norbornene and its derivatives are the most common ROMP monomers, since they combine high reactivity, arising from their high ring strain, with easy synthesis and possibility of introducing desired functional moieties as pendant groups, thus enabling the preparation of advanced polymeric materials for specific applications in biological, chemical, physical, and biomedical fields [23,24,29–35]. To date, several fluorescent tools based on poly(oxa)norbornenes or poly(oxa) norbornene dicarboximides, characterized by various types of fluorescent chromophores in the side chains, have been prepared through ROMP [24,36–42]. Due to the controllability of ROMP process, examples of random copolymers and block copolymers bearing different pendant chromophores have been also reported [43,44].

In order to develop high-performance fluorescent materials, special attention has been paid to the synthesis of nonconiugated polymers having at the same time donor and acceptor chromophores attached to

* Corresponding authors.
E-mail addresses: spragliola@unisa.it (S. Pragliola), fgrisi@unisa.it (F. Grisi).

https://doi.org/10.1016/j.eurpolymj.2023.112539
Received 3 September 2023; Received in revised form 20 October 2023; Accepted 24 October 2023
Available online 27 October 2023

the polymer backbone, able to induce energy, charge, or electron transfer [45–49]. This approach has allowed to construct *via* ROMP highly efficient blue thermally activated delayed fluorescence (TADF) polymers for light-emitting devices [47,48].

In this context, as a part of efforts to develop nonconjugated fluorescent polymers with enhanced optoelectronic properties, some of us recently reported on new fluorescent ROMP polymers based on (oxa) norbornene dicarboximide (**NDI** or **ONDI**) monomers with pendant carbazole or coumarin groups, connected to the polymerizable unit through different spacers (ethylene or *p*-xylene) [50,51]. The interest in using carbazole and coumarin as the fluorophores was mainly related to their easy availability and excellent fluorescence emission, which make them broadly utilized in a variety of functional polymers and materials for different electro-optical applications [52–54], including organic light emitting diodes (OLEDs) [55,56], optical data storages [57–59], or laser dyes [60]. The results gathered during the study suggested that polymer optoelectronic properties can be modulated by appropriate combination of monomer structure and main chain stereochemistry. As a logical extension of this research, we decided to investigate the possibility of preparing, by ROMP, random copolymers containing two distinct functionalities, i.e. carbazole and coumarin, at the same time, with the intention of probing whether copolymer properties could be tuned adjusting and optimizing the fluorophores content into the polymer side chains. In particular, we focused on evaluating possible carbazole-coumarin through-space interactions, as well as their dependence on the copolymer composition. The main aim is to prepare new organic materials for the fabrication of electroluminescent devices that offer advantages such as excellent filmability, high brightness and efficiency, and low cost of fabrication.

To this end, herein we describe the synthesis and characterization of random copolymers from **NDI** monomers bearing pendant carbazole and coumarin moieties, in the presence of the commercial Grubbs catalyst **G3** (Scheme 1), commonly used to promote ROMP reactions in a controlled/living manner [28,61,62]. The synthesis and characterization of a block copolymer with an equal content of carbazole and coumarin is also reported to evaluate the influence of the architecture of copolymers on their fluorescence properties.

2. Experimental section

2.1. Materials

Dichloro[1,3-bis (2,4,6-trimethylphenyl)-2-imidazolidinylidene] (benzylidene)- bis(3-bromopyridine)ruthenium(II) (**G3**) and all reagents and solvents were purchased from Merck Sigma-Aldrich (Italy). The monomers 2-[2-(9H-carbazol-9-yl)ethyl]-3a,4,7,7a-tetrahydro-1H-4,7 methanoisoindole-1,3(2H)-dione (**NDI-EtCar**), 2–4-{[(9H-carbazole-9-yl)methyl]benzyl}-3a,4,7,7a-tetrahydro-1H-4,7- methanoisoindole-1,3 (2H)-dione (**NDI-XyCar**), 3-methylene-2-{2-[(2-oxo-2H-chromen-7-yl) oxy]ethyl}-2,3,3a,4,7,7a-hexahydro-1H-4,7-methanoisoindol-1-one (**NDI-EtCou**), and 2-{4-[((2-oxo-2H-chromen-7-yl)oxy)methyl]benzyl}-3a,4,7,7a-tetrahydro-1H-4,7-methanoisoindole-1,3(2H)-dione (**NDI-XyCou**) were prepared as previously reported [50]. All the operations of synthesis and handling involving air- and moisture-sensitive compounds were performed under dried nitrogen atmosphere by using Schlenk, or glovebox techniques. The glassware and vials used in the polymerization reactions were dried in an oven at 120 °C overnight and subjected to vacuum-nitrogen cycles. Dichloromethane (CH_2Cl_2) was dried refluxing over lithium aluminium hydride ($LiAlH_4$) for 48 h and distilled before use.

2.2. Synthesis of homopolymers and copolymers

2.2.1. Typical homopolymerization procedure

In a glovebox, 0.30 mmol of the appropriate monomer (**NDI-Car** or **NDI-Cou**) were introduced in a vial and dissolved in anhydrous dichloromethane (0.24 M). The vial was taken out from the glove box and warmed to 30 °C. The catalyst **G3** (1.5 μmol) was dissolved in a minimal amount of dichloromethane solution and immediately injected. The reaction mixture was stirred for 20 min. Afterward, the polymerization was quenched with ethyl vinyl ether and kept under stirring for additional 30 min. The product mixture was poured into methanol and the precipitate that formed was collected, redissolved in methylene chloride and reprecipitated in methanol. Then, the obtained polymer was recovered by filtration and dried in a vacuum oven at 40 °C for 12 h.

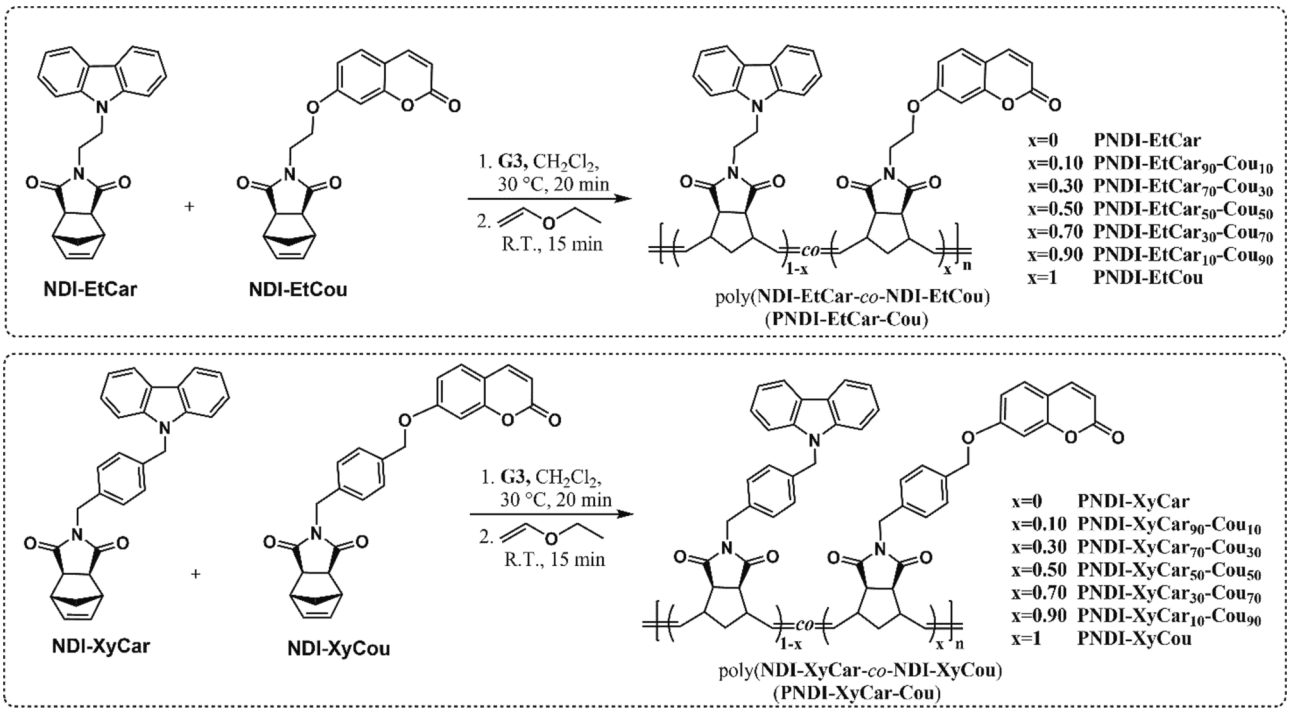

Scheme 1. Synthesis of random copolymers poly(**NDI-EtCar-Cou**) and poly(**NDI-XyCar-Cou**).

The NMR, UV–Vis and fluorescence spectroscopic data for all the homopolymers matched with those previously reported. [50].

2.2.2. Typical random copolymerization procedure

In a glovebox, the appropriate comonomers **NDI-Car** and **NDI-Cou** (different ratios, 0.30 mmol total amount) were dissolved in anhydrous dichloromethane (0.24 M). The vial was taken out from the glove box and warmed to 30 °C. **G3**, dissolved in a minimal quantity of anhydrous dichloromethane, was immediately injected and the reaction mixture was stirred for 20 min. The reaction was then quenched with ethyl vinyl ether and kept under stirring for additional 30 min. Subsequently, the product mixture was poured in methanol to precipitate out the crude copolymer. The latter was collected via filtration, redissolved in methylene chloride, reprecipitated in methanol and then dried at 40 °C under reduced pressure for 12 h.

2.2.3. Block copolymerization procedure

The monomer **NDI-Et-Car** (0.15 mmol), chosen for the synthesis of the first block, was dissolved in anhydrous dichloromethane (0.24 M) into a 5 mL Schlenk tube, and the solution was warmed at 30 °C. **G3** was then dissolved in a minimal amount of anhydrous dichloromethane and immediately added to the monomer solution. The reaction mixture was kept stirring for 20 min, then a solution of **NDI-EtCou** (0.15 mmol, 0.24 M) was added and the polymerization reaction was left under stirring for additional 20 min. After this time, an excess of ethyl vinyl ether was added to terminate ROMP reaction. The mixture was stirred for 30 min, and then poured into an excess of methanol. The crude copolymer was collected, redissolved in dichloromethane, and then added to an excess of methanol once again. The obtained polymer was dried in a vacuum oven at 40 °C for 12 h.

2.3. Characterization

1D and 2D NMR spectra were recorded on a BRUKER ASCEND 600 spectrometer (600 MHz for ^{1}H; 150 MHz for ^{13}C) operating at 298 K. The samples were prepared by dissolving 15–20 mg of polymer in 0.5 mL of deuterated chloroform ($CDCl_3$). Tetramethylsilane (TMS) was used as internal chemical shift reference.

Molecular masses (M_n and M_w) and dispersities ($Đ$) were measured by gel permeation chromatography (GPC) at 30 °C, using $CHCl_3$ as the eluent (1 mL/min) and narrow polystyrene standards as reference. The measurements were performed on an Agilent GPC/SEC instrument using a PLgel 5 μm MIXED-C, 7.5 × 300 mm column (p/n PL1110-6500), Linear MW Operating Range: 200 to 2,000,000 g/mol (PS equiv).

Thermogravimetric analysis (TGA) measurements were performed on a TGA Q500 apparatus in flowing N_2 (100 cm^3/min). 5 mg of each polymer were placed in platinum pans and heated in the range 20–800 °C at a rate of 10 °C/min.

Differential scanning calorimetry (DSC) measurements were performed using a TA DSC Q20 instrument in flowing N_2. Polymer samples of 5–7 mg were placed in aluminum pans and heated/cooled at a rate of 10 °C/min. Measurements were done in the range 0–250 °C.

Ultraviolet–visible (UV–Vis) measurements were performed by an Agilent Varian Cary 50 spectrophotometer and photoluminescence recorded by an Agilent Varian Cary Eclipse spectrophotometer. Thin polymer films were prepared by spin coating (chloroform was used as solvent) on quartz slide substrate. The solutions (1 mg/10 mL) have been spin coated in air at 500 rpm for 60 s. The film thicknesses were 100 nm.

The fluorescence quantum yields of the polymers were measured in dilute $CHCl_3$ solution (1 mg/10 mL) using quinine sulfate (0.55 in 0.1 M H_2SO_4) as standard. Values were calculated according to the following equation:

$$Q_s = Q_r(A_r/A_s)(E_s/E_r)(n_s/n_r)^2$$

where Q_s is the quantum yield of the sample, Q_r is the quantum yield of the standard, A_r and A_s are the absorbances of the sample and the standard at the excitation wavelength (290 nm), respectively, E_s and E_r are the integrated emission intensities of the sample and the standard respectively, and n_s and n_r are the refractive indexes of the corresponding solutions (pure solvents ($CHCl_3$ and H_2O) were assumed). The quantum yields of all polymers are listed in Table S1 of S.I..

3. Results and discussion

3.1. Synthesis and characterization of copolymers

The chemical structures of the norbornene dicarboximide (**NDI**) monomers functionalized with carbazole and coumarin fluorophores are depicted in Scheme 1. **NDI-EtCar**, **NDI-EtCou**, **NDI-XyCar** and **NDI-XyCou** were prepared and characterized as previously described [50,63].

The couples of **NDI** monomers with the same spacer (ethylene or xylene) were readily copolymerized by ROMP, in dichloromethane at 30 °C, using the third-generation Grubbs catalyst (**G3**) to give the related random copolymers poly(**NDI-EtCar**-*co*-**NDI-EtCou**) (**PNDI-EtCar-Cou**) and poly(**NDI-XyCar**-*co*-**NDI-XyCou**) (**PNDI-XyCar-Cou**), as illustrated in Scheme 1. The comonomers:catalyst molar ratio was 200:1 in all of them, while the feed molar ratios of **NDI-Car** and **NDI-Cou** monomers were 90:10, 70:30, 50:50, 30:70 and 10:90, respectively. According to the feed molar ratio of the comonomers, the copolymers containing the ethylene bridge are named as **PNDI-EtCar$_{90}$-Cou$_{10}$**, **PNDI-EtCar$_{70}$-Cou$_{30}$**, **PNDI-EtCar$_{50}$-Cou$_{50}$**, **PNDI-EtCar$_{30}$-Cou$_{70}$**, **PNDI-EtCar$_{10}$-Cou$_{90}$**, respectively. Analogously, the polymer samples obtained from the monomers with the xylene bridge, are titled as **PNDI-XyCar$_{90}$-Cou$_{10}$**, **PNDI-XyCar$_{70}$-Cou$_{30}$**, **PNDI-XyCar$_{50}$-Cou$_{50}$**, **PNDI-XyCar$_{30}$-Cou$_{70}$**, **PNDI-XyCar$_{10}$-Cou$_{90}$**, respectively.

The homopolymers **PNDI-EtCar**, **PNDI-EtCou**, **PNDI-XyCar** and **PNDI-XyCou** were also synthesized for comparison. The polymerization results are summarized in Table 1. Polymerizations were interrupted after 20 min and the extent of monomer conversion to polymer was evaluated from ^{1}H NMR spectra of crude polymerization mixtures. Full conversions were observed in all cases, as revealed by the complete disappearance of the monomer olefinic signals in the range 6.23–6.27 ppm, and the appearance of the polymer chain olefinic signals (*cis* and *trans*) in the range 5.18–5.83 ppm [50]. As observed in the synthesis of related homopolymers [50], the nature of the spacer (ethylene or *p*-xylene) in the **NDI** monomers seems to have no influence on the polymerization outcome.

The copolymer microstructures were investigated using 1D and 2D NMR spectroscopy, and the ^{1}H, ^{13}C and HSQC NMR spectra of all the copolymer samples are reported in the Supporting Info (Figure S1-S32). Representative ^{1}H NMR spectra of copolymers **PNDI-EtCar$_{50}$-Cou$_{50}$** and **PNDI-XyCar$_{50}$-Cou$_{50}$**, obtained using a 50:50 comonomer feed ratio, are shown in Fig. 1. For comparison, the ^{1}H NMR spectra of the related homopolymers are also reported. The compositions of all copolymers **PNDI-EtCar-Cou** were determined from ^{1}H NMR spectra by correlating the relative intensities of the resonance of the coumarin proton **o**, centered at 6.14 ppm, and the resonance relative to the carbazole protons **j**, centered at 8.04 ppm (Fig. 1 and Figure S16). For copolymers of the **PNDI-XyCar-Cou** series, the percentages of comonomers in the polymer chain were estimated from the integration ratios of the same diagnostic signals, resonating at 6.14 ppm for the coumarin proton **q** and at 8.06 ppm for the carbazole protons **l** (Fig. 2 and Figure S32). The final contents of comonomers in the polymer chains are in excellent agreement with the initial comonomer feed ratios (see Table 1).

Concerning the stereochemistry of the double bonds in the main chain, in the **PNDI-EtCar-Cou** series the overlap of the olefinic diagnostic signals in the ^{1}H NMR spectra at 5.86–5.16 ppm prevented the determination of the *cis/trans* ratios, which were estimated by

Table 1
Results of ROMP homo- and copolymerization of **NDI-Car** and **NDI-Cou** promoted by **G3.**

Polymer[a]	NDI-Car (mmol)	NDI-Cou (mmol)	NDI-Cou[b] (%)	M_n[c] (kDa)	$Đ$[c]	T_d[d] (°C)	T_g[e] (°C)	$T_{g,th}$[f] (°C)
PNDI-EtCar	0.30	0.00	0	53.0	1.09	410	190	–
PNDI-EtCar$_{90}$-Cou$_{10}$	0.27	0.03	8.9	53.2	1.13	428	186	186
PNDI-EtCar$_{70}$-Cou$_{30}$	0.21	0.09	25.5	63.4	1.23	419	176	176
PNDI-EtCar$_{50}$-Cou$_{50}$	0.15	0.15	45.9	62.9	1.22	403	165	166
PNDI-EtCar$_{30}$-Cou$_{70}$	0.09	0.21	69.0	64.2	1.26	414	156	154
PNDI-EtCar$_{10}$-Cou$_{90}$	0.03	0.27	89.3	68.0	1.25	379	148	144
PNDI-EtCou	0.00	0.30	100	51.6	1.11	392	140	–
PNDI-XyCar	0.30	0.00	0	65.6	1.15	394	195	–
PNDI-XyCar$_{90}$-Cou$_{10}$	0.27	0.03	9.5	68.4	1.23	385	188	190
PNDI-XyCar$_{70}$-Cou$_{30}$	0.21	0.09	27.8	80.5	1.37	360	179	181
PNDI-XyCar$_{50}$-Cou$_{50}$	0.15	0.15	50.0	77.8	1.25	358	169	170
PNDI-XyCar$_{30}$-Cou$_{70}$	0.09	0.21	69.8	85.0	1.29	365	161	161
PNDI-XyCar$_{10}$-Cou$_{90}$	0.03	0.27	91.4	69.4	1.22	367	152	152
PNDI-XyCou	0.00	0.30	100	64.4	1.16	366	145	–
P(NDI-EtCar-*b*-NDI-EtCou)	0.15	0.15	49.5	51.8	1.30	391	147, 189	–

[a] Reaction conditions: comonomers (0.30 mmol) and catalyst (1.5 μmol) in CH_2Cl_2 (1.25 mL, 0.24 M) at 30 °C for 20 min. For the synthesis of the block copolymer **P(NDI-EtCar-*b*-NDI-EtCou)**, the reaction time was 40 min.
[b] Determined by ^{1}H NMR analysis of the purified polymer.
[c] Determined by GPC relative to polystyrene standards in $CHCl_3$.
[d] Evaluated by TGA at 5% weight loss.
[e] Determined from the second heating run at heating rate of 10 °C min^{-1}.
[f] Theoretical values calculated by Fox equation [64] according to the literature reported.

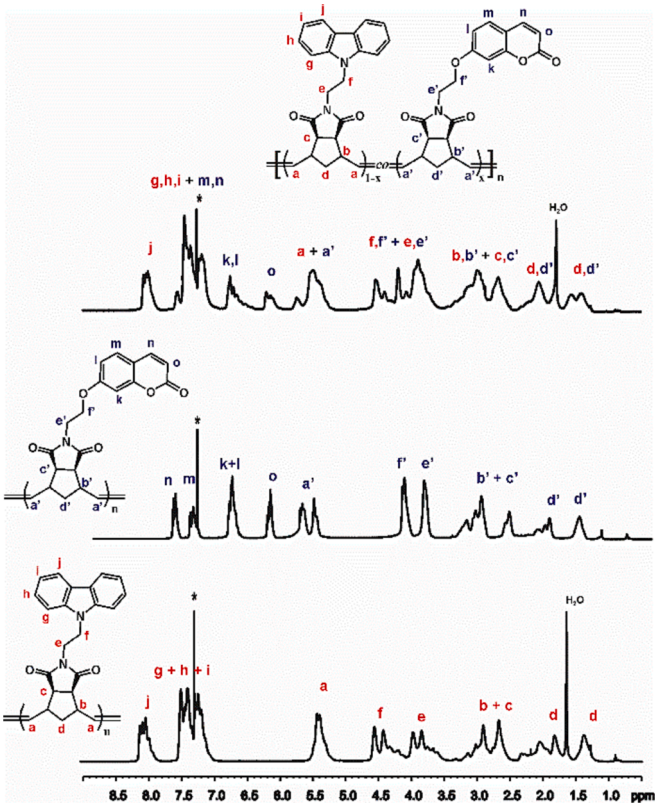

Fig. 1. ^{1}H NMR spectra (600 MHz, $CDCl_3$) of poly(**NDI-EtCar$_{50}$-Cou$_{50}$**), poly(**NDI-EtCou**), poly(**NDI-EtCar**). The asterisk denotes the residual protio impurity of the solvent.

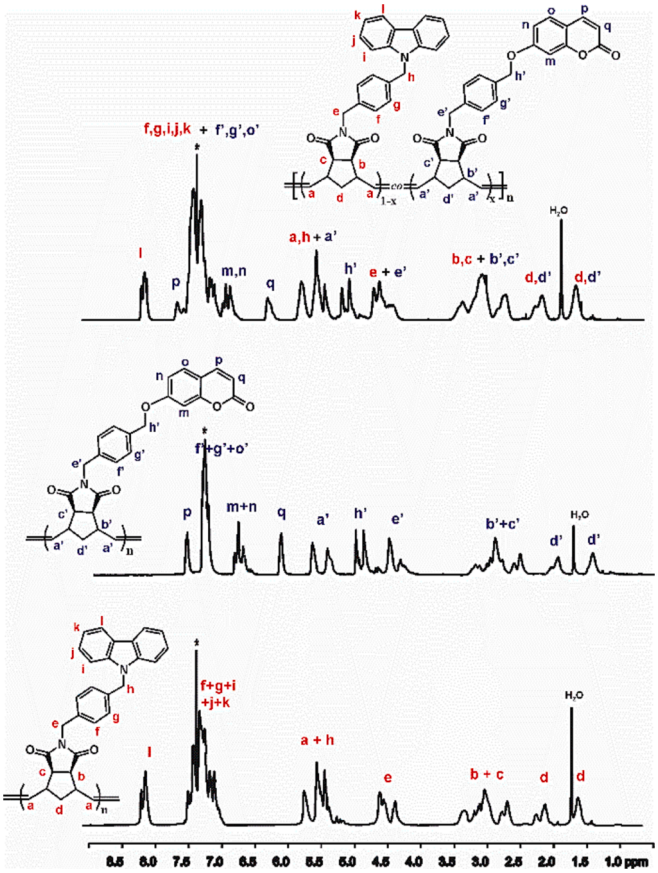

Fig. 2. ^{1}H NMR spectra (600 MHz, $CDCl_3$) of poly(**NDI-XyCar$_{50}$-Cou$_{50}$**), poly(**NDI-XyCou**), poly(**NDI-XyCar**). The asterisk denotes the residual protio impurity of the solvent.

integrating the olefin carbons resonating in the region 134.43–132.48 ppm (*cis*) and 132.45–131.10 ppm (*trans*) in the ^{13}C NMR spectra (see SI). A slight prevalence of *trans* linkages was observed, with percentages varying from 57 to 60 %. In the **PNDI-XyCar** series, due to the overlap of the copolymer olefinic signals at 5.78–5.19 ppm with the ones relative to the methylene protons linked to the carbazole unit, the content of *cis/trans* sequences were calculated by the integration of ^{13}C NMR diagnostic signals observed in the region 134.37–132.33 ppm (*cis*) and 132.32–131.32 ppm (*trans*) (see SI). The percentages of *trans* double bonds were found to be in the range 58–61 %.

GPC analysis results show that the ROMP copolymerization proceeds in a controlled fashion, as typically observed for polymerization reactions promoted by **G3** [28]. All copolymers display monomodal molecular weight distributions and low dispersities ($1.09<Đ<1.37$). The experimental M_n values of copolymers are in reasonable agreement with the theoretical ones [65], falling in the range $70.3 < M_n < 71.3$ kDa for the **PNDI-EtCar-Cou** series and in the range $85.5 < M_n < 86.5$ kDa for the **PNDI-XyCar-Cou** series, since the observed deviations could be ascribed to differences between the structures of the target polymers and the polystyrene standards used for molecular weights measurements.

Considering the good polymerization control registered in the synthesis of random copolymers of **NDI-Car** and **NDI-Cou** monomers by ROMP, we turned our attention towards the possibility of preparing block copolymers in the same way. In this view, the synthesis of block copolymer **P(NDI-EtCar-*b*-NDI-EtCou)** was attempted by sequential addition of **NDI-EtCar** and **NDI-EtCou**, using a comonomer ratio 50:50 (see Table 1). Also in this case, ^{1}H NMR analysis on the crude polymerization mixture revealed complete conversions of both monomers. The copolymer composition is in excellent agreement with the comonomer feed ratio, as determined from ^{1}H NMR spectrum (Figure S33). The successful formation of the block copolymer was proven by 2D DOSY NMR experiment (Figure S36) and GPC analysis. According to the DOSY map, **PNDI-EtCar** and **PNDI-EtCou** sequences in the polymer chain exhibit the same diffusion coefficient of 6.92×10^{-12} m^2/s, as would be expected for an efficient copolymerization of related monomers. Consistently, the GPC trace shows a monomodal molecular weight distribution.

The thermal properties of **PNDI-EtCar-Cou** and **PNDI-XyCar-Cou** copolymers were investigated by thermogravimetric analysis (TGA) and differential scanning calorimetry (DSC). The thermal behaviour of **PNDI-EtCar**, **PNDI-EtCou**, **PNDI-XyCar** and **PNDI-XyCou** homopolymers was reported for comparison.

As shown in Table 1, all the copolymers showed excellent thermal stability with decomposition temperatures (T_d, with 5 % weight loss) in the range 358–428 °C (see SI). A clear glass transition temperature (T_g) is observed for each polymer with values ranging from 148 to 186 °C for the **PNDI-EtCar-Cou** series (Fig. 3a) and from 152 to 188 °C for the **PNDI-XyCar-Cou** series (Fig. 3b).

No peaks that could be associated with crystallization or melting were detected, suggesting amorphous morphologies across both the series of copolymers. The differences in T_d and T_g values are very small, suggesting that the nature of the linker (ethylene or *p*-xylene) between the main chain and the pendant units of the copolymers does not influence their thermal properties.

The T_g's of all random copolymers are plotted as a function of their **NDI-Cou** content in Fig. 4. As it can be observed, the T_g varies continuously with copolymer composition for both the series of copolymers and closely follows the trend of the values predicted using the Fox equation, thus indicating a good miscibility between the monomer units of both the copolymer series.

As expected, the block copolymer **P(NDI-EtCar-*b*-NDI-EtCou)** tends to show phase separation and displays two glass transitions, corresponding to T_g for each type of block (Figure S52).

3.2. Optical characterization

A preliminary study of the optical properties of both copolymer series, **PNDI-EtCar-Cou** and **PNDI-XyCar-Cou**, was conducted. The analysis of absorption spectra of all copolymers was performed for $CHCl_3$ solutions and, in the solid state, for films. The UV–vis spectrum of each copolymer sample (Figures S53-S63) includes both the two distinctive bands in the region from 300 nm to 355 nm of the carbazole rings [66] and the broad band presenting a maximum at 322 nm characteristic of the coumarin group [67]. As an example, in Fig. 5, the UV–vis spectra of **PNDI-EtCar$_{50}$-Cou$_{50}$** (**a,b**) and **PNDI-XyCar$_{50}$-Cou$_{50}$** (**c,d**) samples are depicted. For comparison, **PNDI-EtCar**, **PNDI-EtCou**, **PNDI-XyCar** and **PNDI-XyCou** homopolymer spectra are also showed.

The emission spectra of all **PNDI-EtCar-Cou** copolymer samples, both in $CHCl_3$ solution and in the solid state as films, were recorded at room temperature by using an excitation wavelength of 290 nm. In Fig. 6, the solution emission spectra of **PNDI-EtCar-Cou** copolymers and those of the homopolymers **PNDI-EtCar** and **PNDI-EtCou** are showed. As already reported by some of us [50], **PNDI-EtCar** solution spectrum presents two bands at Λ_{max} = 352 and 366 nm assignable to isolated carbazole group emission, as well as **PNDI-EtCou** spectrum shows a broad band peaked at 387 nm due to the coumarin group emission. As for the emission spectra of **PNDI-EtCar-Cou** copolymers, they present together with the typical bands of both carbazole and coumarin groups, a broad band at 450 nm whose intensity depends on the **NDI-EtCar**/**NDI-EtCou** ratio in the copolymer chains. In detail, the band intensity increases as the content of coumarin groups (**NDI-EtCou** units) in the copolymers decreases (see the inset of Fig. 6).

Consisting with already reported in literature for copolymers bearing both carbazole and coumarine pendant groups [68], the origin of this new band at 450 nm can be attributed to an energy transfer phenomenon from the fluorescent emitter carbazole groups to the lower energy acceptor coumarin groups. As showed in Fig. 7, the overlap, albeit partial, between the **NDI-EtCar** monomer photoluminescence spectrum and the **NDI-EtCou** monomer absorption spectrum, as well as between those of **PNDI-EtCar** and **PNDI-EtCou** homopolymers, strongly suggests that **PNDI-EtCar-Cou** copolymers may undergo to energy transfer from carbazole to coumarin groups.

In Fig. 8, the emission solution spectrum of the **PNDI-EtCar$_{50}$-Cou$_{50}$** copolymer sample and those of the **PNDI-EtCar/PNDI-EtCou** 50/50

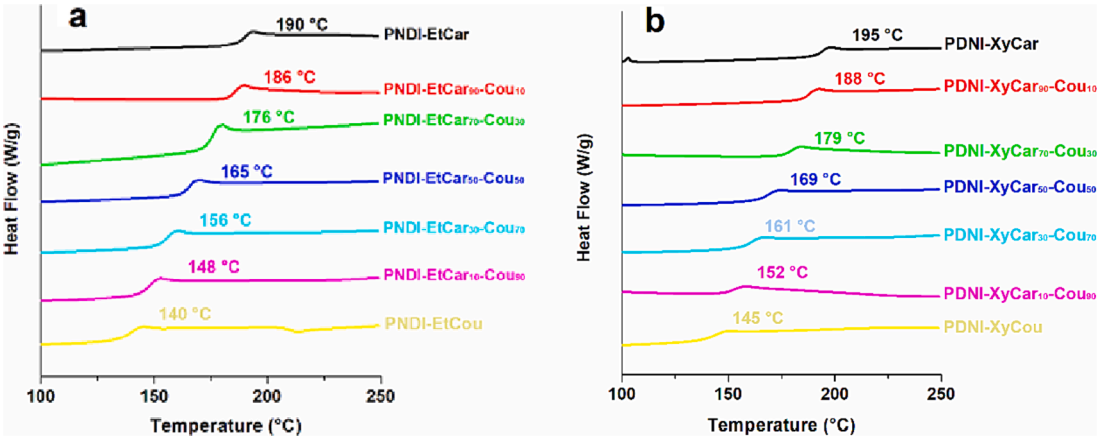

Fig. 3. DSC curves (second heating run) of **PNDI-EtCar-Cou**, **PNDI-EtCar**, **PNDI-EtCou** (**a**), and **PNDI-XyCar-Cou**, **PNDI-XyCar**, **PNDI-XyCou** (**b**).

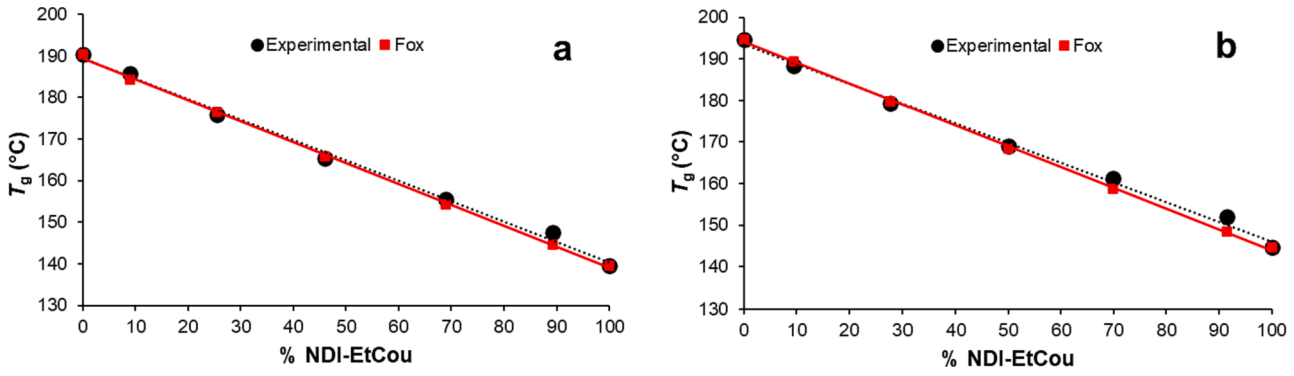

Fig. 4. Experimental T_g values compared with those obtained by Fox equation for poly(**NDI-EtCar-Cou**) (**a**) and poly(**NDI-XyCar-Cou**) (**b**) series.

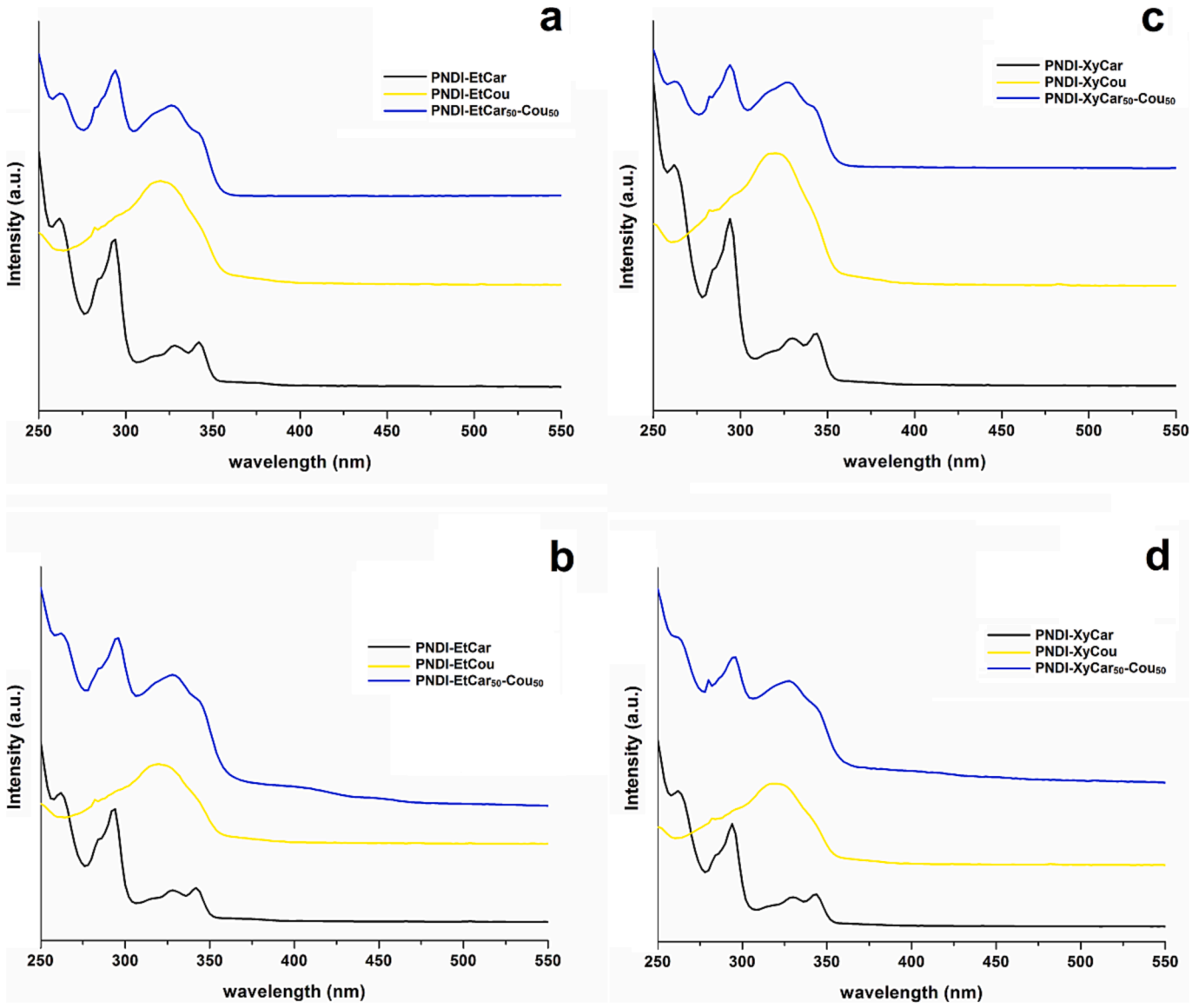

Fig. 5. Absorption spectra of **PNDI-EtCar$_{50}$-Cou$_{50}$, PNDI-EtCar, PNDI-EtCou, PNDI-XyCar$_{50}$-Cou$_{50}$, PNDI-XyCar and PNDI-XyCou** (**a** and **c**: 1 mg/10 mL $CHCl_3$ solution spectra, **b** and **d**: thin film spectra).

homopolymer blend and the **P(NDI-EtCar-*b*-NDI-EtCou)** block copolymer samples are compared. Both **PNDI-EtCar/PNDI-EtCou 50/50** homopolymer blend and **P(NDI-EtCar-*b*-NDI-EtCou)** block copolymer spectra have the same shape resulting from the sum of **PNDI-EtCar** and **PNDI-EtCou** emission. No band at 450 nm, which is instead prevailing in the **PNDI-EtCar$_{50}$-Cou$_{50}$** spectrum, is detected. These experimental results clearly indicate that in dilute solution conditions, the energy transfer from the donor carbazole group to the acceptor coumarin group

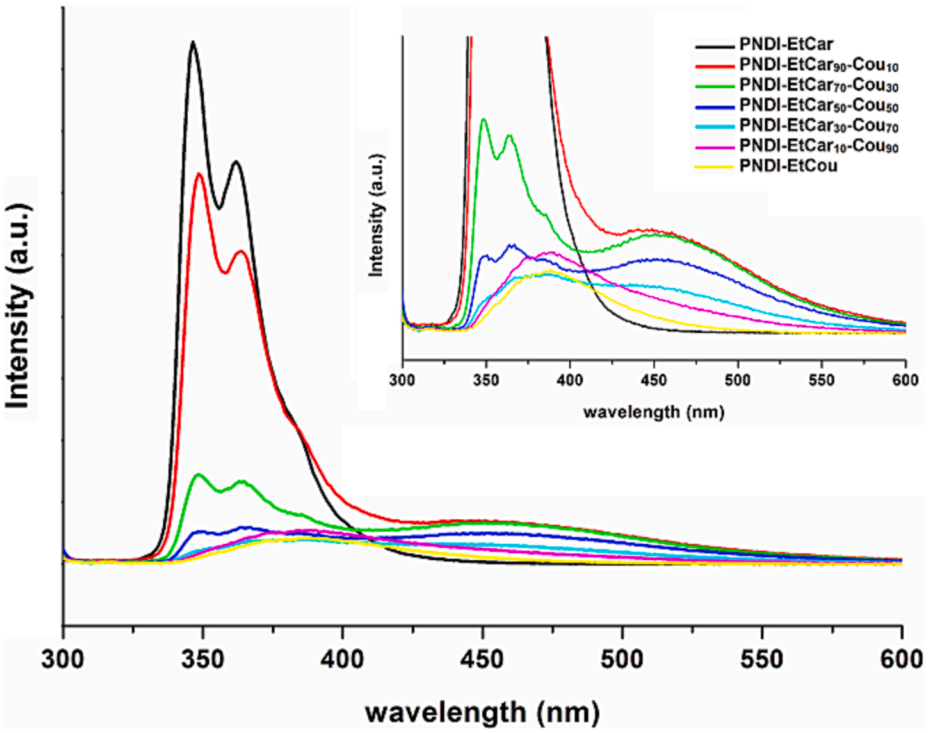

Fig. 6. Emission spectra of 1 mg/10 mL $CHCl_3$ solution of **PNDI-EtCar-Cou** copolymers, **PNDI-EtCar** and **PNDI-EtCou** homopolymers. Λ_{ecc} = 290 nm.

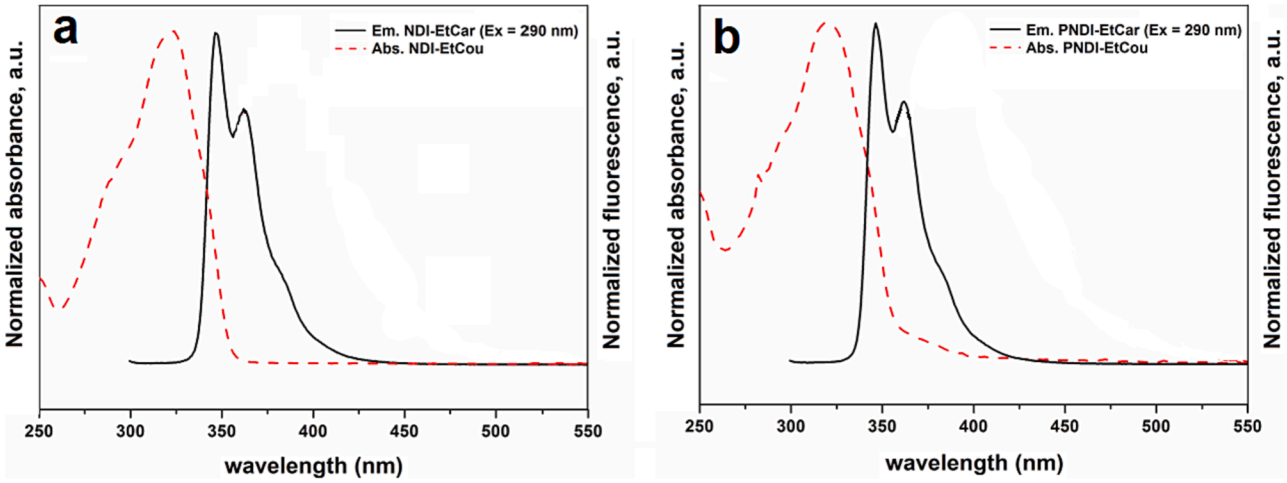

Fig. 7. Absorption and emission spectra of 1 mg/10 mL $CHCl_3$ solution of **NDI-EtCou** and **NDI-EtCar** (left) and **PNDI-EtCou** and **PNDI-EtCar** (right).

is an intramolecular phenomenon and can probably occur between carbazole and coumarin groups belonging either to adjacent monomer units of the same copolymer chain, or eventually, due to the folding of the copolymer chain, to more distant units. This is also consistent with the decrease of the 450 nm band intensity observed with increasing content of coumarin groups in the polymer chains. In fact, since **PNDI-EtCar-Cou$_s$** are random copolymers, the probability that an **NDI-EtCou** unit is neighboring to an **NDI-EtCar** unit in the same polymer chain should increase as the number of **NDI-EtCou** units decreases.

Fig. 9 shows the emission spectra of all **PNDI-EtCar-Cou** copolymer samples in the solid state as films and, for comparison, those of **PNDI-EtCar** and **PNDI-EtCou** homopolymers, **PNDI-EtCar/PNDI-EtCou 50/50** homopolymer blend and, **P(NDI-EtCar-*b*-NDI-EtCou)** block copolymer, too. Although a slight red shift is detected, both **PNDI-EtCar** and **PNDI-EtCou** homopolymers show spectral profiles like those of solution ones.

Differently, all **PNDI-EtCar-Cou** copolymer samples as well as the **PNDI-EtCar/PNDI-EtCou 50/50** homopolymer blend and the **P(NDI-EtCar-*b*-NDI-EtCou)** block copolymer ones show very similar film spectra presenting a broad band in the 350–500 nm region. These experimental results seem to suggest that in the solid state, the close packing of polymer chains allows the energy transfer from the donor carbazole groups to the acceptor coumarin groups not only through intrachain interactions, but also through interchain interactions. In fact, also the **PNDI-EtCar/PNDI-EtCou 50/50** homopolymer blend and the **P(NDI-EtCar-*b*-NDI-EtCou)** block copolymer film spectra have only one broad band in the 350–500 nm region which is instead completely missing in their solution spectra, while the emission of the donor carbazole groups is completely quenched.

It is worth noting that the broad band in the 350–500 nm region of the **PNDI-EtCar-Cou** film emission spectra is peaked at about 420 nm and blue shifted respect to the solution ones. This could be justified

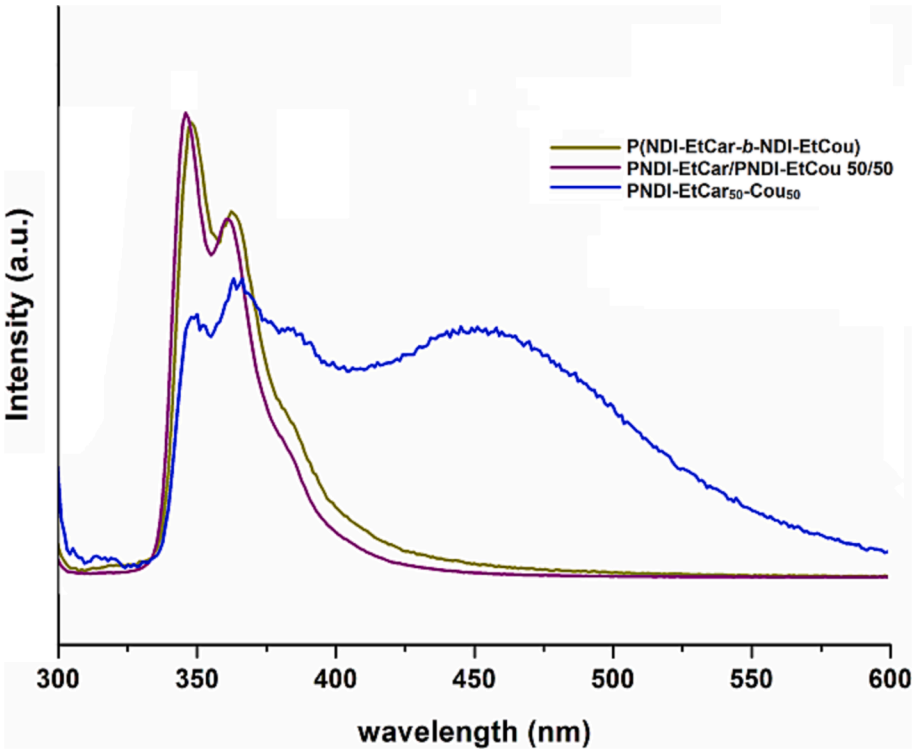

Fig. 8. Emission spectra of 1 mg/10 mL $CHCl_3$ solution of **PNDI-EtCar$_{50}$-Cou$_{50}$, PNDI-EtCar/PNDI-EtCou 50/50** homopolymer blend and **P(NDI-EtCar-*b*-NDI-EtCou)** block copolymer. $\Lambda_{ecc} = 290$ nm.

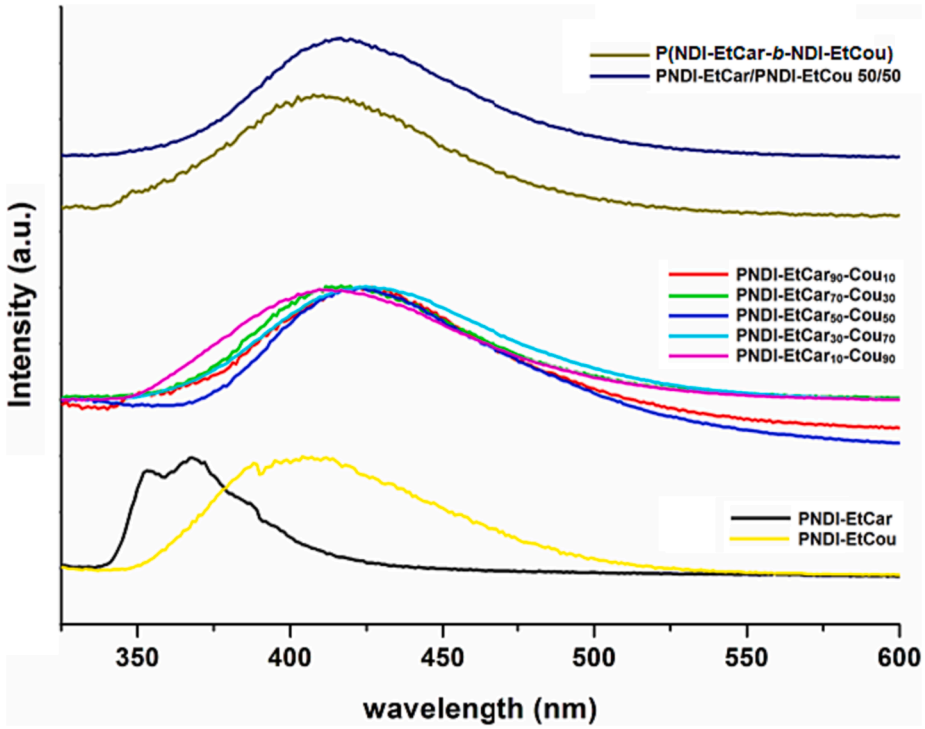

Fig. 9. Emission spectra of films of **PNDI-EtCar, PNDI-EtCou, PNDI-EtCar-Cou** copolymers, **PNDI-EtCar/PNDI-EtCou 50/50** homopolymer blend and **P(NDI-EtCar-*b*-NDI-EtCou)** block copolymer. $\Lambda_{ecc} = 290$ nm.

hypothesizing that the broadened band in the 350–500 nm region, both in the solution and film spectra, originates not only from the energy transfer but also, from the electron transfer from the donor carbazole groups to the acceptor coumarin groups [69,70]. This means that both energy and electron transfer phenomena could contribute to the formation of the band. The electron transfer could involve lower energies and be favored by the solvent polarity, so to justify the observed red shift in the solution spectra of **PNDI-EtCar-Cou** respect to the film ones. To

support this suggestive hypothesis **PNDI-EtCar$_{50}$-Cou$_{50}$** emission spectra were recorded in solvents of varying polarities (see Figure S64 in S.I.). A blue shift of the 350–500 nm region band is observed in the spectra recorded in lower polarity solvents (toluene and heptane) respect to chloroform. Although these data are only preliminary, they seem to confirm the hypothesis that electron transfer phenomena from the carbazole donor to the coumarin acceptor in our copolymers may be induced by polar solvents. Currently, further and deeper studies are underway to better understand the optical behavior of these copolymers.

To investigate the possible influence of the nature of the linker (ethylene or *p*-xylene) on copolymers fluorescence behaviour, the emission spectra of **PNDI-XyCar-Cou** copolymer series, both in solution (figure S65a) and in the solid state as films (Figure S65b), were also analyzed.

Fluorescence properties of **PNDI-XyCar-Cou** copolymers basically do not differ from those of **PNDI-EtCar-Cou** copolymers, indicating no substantial effect due to the replacement of a flexible spacer (ethylene) with a more rigid one (*p*-xylene).

4. Conclusions

In this work, novel random copolymers presenting carbazole and coumarin as pendant fluorophore groups, connected to a poly(norbornene dicarboximide) skeleton by an ethylene or *p*-xylene spacer, were prepared by ROMP in the presence of commercial Grubbs' catalyst **G3**. The successful incorporation of the two fluorophores in both the series of copolymers, in the desired relative ratios, was confirmed by ^{1}H NMR analysis. Consistent with a controlled polymerization mechanism, all the obtained copolymer samples showed monomodal molecular weight distributions and low dispersities. Thanks to the possibility of controlling the ROMP process, a block copolymer containing an equal amount of carbazole and coumarin monomer sequences was successfully synthesized. All the copolymers displayed high thermal stabilities and possessed an amorphous nature. Moreover, for the two series of random copolymers, the T_g values were strictly dependent on the copolymer composition, decreasingly linearly and in a well-controlled manner as the coumarin content in the copolymer was increased.

As for fluorescence behaviour, the emission spectra of each copolymer showed, together with the typical bands of carbazole and coumarin groups, a broad band centered at 450 nm that can be attributed to an energy transfer phenomenon from the donor carbazole groups to the acceptor coumarin groups, and whose intensity depends on the copolymer composition and decreases with the increasing of the coumarin amount in the copolymers. This additional band was not observed in the emission spectra of the block copolymer as well as of a blend 50/50 of the two related homopolymers, suggesting that the energy transfer occurs through intramolecular interactions. The analysis of the emission spectra of copolymers films, instead, seems to indicate that the energy transfer in the solid state takes place not only through intrachain interactions, but also through interchain interactions. Moreover, with respect to the solution spectra, a blue shift of the additional band from 450 at 420 nm was observed, probably due to a combined effect of both energy and electron transfer phenomena. As a general remark, the results of this study highlight the influence of copolymers architecture and composition in modulating the energy transfer between the fluorescent donor and acceptor groups, that can result in enhanced fluorescence properties. These features, together with the high thermal stabilities and good filmability of the copolymers, can be exploited for the development of electroluminescent devices. Further investigations are ongoing to completely explain the observed copolymers fluorescence behaviour and will be reported in the due course.

CRediT authorship contribution statement

Mario Carratù: Investigation, Data curation, Formal analysis. **Rubina Troiano:** Investigation, Data curation, Formal analysis. **Chiara Costabile:** Formal analysis, Funding acquisition. **Antonella Caterina Boccia:** Data curation, Formal analysis. **Stefania Pragliola:** Data curation, Resources, Formal analysis, Resources, Writing – original draft, Writing – review & editing. **Fabia Grisi:** Conceptualization, Methodology, Data curation, Resources, Formal analysis, Resources, Supervision, Writing – original draft, Writing – review & editing.

Declaration of Competing Interest

The authors declare that they have no known competing financial interests or personal relationships that could have appeared to influence the work reported in this paper.

Data availability

Data will be made available on request.

Acknowledgements

The authors thank Drs. Patrizia Oliva, Ivano Immediata and Mariagrazia Napoli for the technical support and Michele Polise for some experimental work. The authors are grateful for funding from the Università degli Studi di Salerno (FARB grants) and from PON program ARS01_01088 2018-2021.

Appendix A. Supplementary data

Supplementary data to this article can be found online at https://doi.org/10.1016/j.eurpolymj.2023.112539.

References

[1] T. Ueno, T. Nagano, Fluorescent probes for sensing and imaging, Nat. Methods 8 (2011) 642–645, https://doi.org/10.1038/nmeth.1663.
[2] Y. Yang, F. Gao, Y. Wang, H. Li, J. Zhang, Z. Sun, Y. Jiang, Fluorescent Organic Small Molecule Probes for Bioimaging and Detection Applications, Molecules 27 (2022) 8421, https://doi.org/10.3390/molecules27238421.
[3] X. Lu, Y. Zhan, W. He, Recent development of small-molecule fluorescent probes based on phenothiazine and its derivates, J. Photochem. Photobiol. B Biol. 234 (2022), 112528, https://doi.org/10.1016/j.jphotobiol.2022.112528.
[4] J. Chan, S. Dodani, S., C. Chang,, Reaction-based small-molecule fluorescent probes for chemoselective bioimaging, Nature Chem 4 (2012) 973–984, https://doi.org/10.1038/nchem.1500.
[5] T. Terai, T. Nagano, Fluorescent probes for bioimaging applications, Curr. Opin. Chem. Biol. 12 (2008) 515–521, https://doi.org/10.1016/j.cbpa.2008.08.007.
[6] Y. You, Y. He, P.E. Burrows, S.R. Forrest, N.A. Petasis, M.E. Thompson, Fluorophores Related to the Green Fluorescent Protein and Their Use in Optoelectronic Devices, Adv. Mater. 12 (2000) 1678–1681, https://doi.org/10.1002/1521-4095(200011)12:22<1678::AID-ADMA1678>3.0.CO;2-H.
[7] O. Ostroverkhova, Organic Optoelectronic Materials: Mechanisms and Applications, Chem. Rev. 116 (2016) 13279–13412, https://doi.org/10.1021/acs.chemrev.6b00127.
[8] G. Ahumada, M. Borkowska, Fluorescent Polymers Conspectus, Polymers 14 (2022) 1118, https://doi.org/10.3390/polym14061118.
[9] A. Alvarez, J.M. Costa-Fernández, R. Pereiro, A. Sanz-Medel, A. Salinas-Castillo, Fluorescent conjugated polymers for chemical and biochemical sensing, TrAC Trends Anal. Chem. 30 (2011), https://doi.org/10.1016/j.trac.2011.04.017.
[10] A. Jose, A. Tharayil, M. Porel, Water soluble non-conjugated fluorescent polymers: aggregation induced emission, solid-state fluorescence, and sensor array applications, Polym. Chem. 14 (2023) 3309–3316, https://doi.org/10.1039/D3PY00357D.
[11] Q. Bu, P. Li, Y. Xia, D. Hu, W. Li, D. Shi, K. Song, Design, Synthesis, and Biomedical Application of Multifunctional Fluorescent Polymer Nanomaterials, Molecules 28 (2023) 3819, https://doi.org/10.3390/molecules28093819.
[12] M. Sawamoto, J. Fujimori, T. Higashimura, Living Cationic Polymerization of iV-Vinylcarbazole Initiated by Hydrogen Iodide, Macromolecules 20 (1987) 916–920, https://doi.org/10.1021/ma00171a003.
[13] B. Zhao, H. Ma, C. Wang, Z. Shang, Y. Ding, A. Hu, Silicon Promoted Cationic Polymerization of Phenylacetylenes, Macromolecules 53 (2020) 240–248, https://doi.org/10.1021/acs.macromol.9b02191.
[14] J.-D. Tong, S. Ni, M.A. Winnik, Synthesis of Polyisoprene-b-Polystyrene Block Copolymers Bearing a Fluorescent Dye at the Junction by the Combination of Living Anionic Polymerization and Atom Transfer Radical Polymerization, Macromolecules 33 (2000) 1482–1486, https://doi.org/10.1021/ma990682e.

[15] X. Ji, W. Tian, K. Jin, H. Diao, G. Song, J. Zhang, Anionic polymerization of nonaromatic maleimide to achieve full-color nonconventional luminescence, Nat. Commun. 13 (2022) 3717, https://doi.org/10.1038/s41467-022-31547-2.

[16] N. Haridharan, R. Dhamodharan, Controlled polymerization of carbazole-based vinyl and methacrylate monomers at ambient temperature: A comparative study through ATRP, SET, and SET-RAFT polymerizations, J. Polym. Sci. A Polym. Chem. 49 (2011) 1021–1032, https://doi.org/10.1002/pola.24518.

[17] K. He, S. Chen, W. Xu, X. Tai, Y. Chen, P. Sun, Q. Fan, W. Huang, High-stability NIR-II fluorescence polymer synthesized by atom transfer radical polymerization for application in high-resolution NIR-II imaging, Biomater. Sci. 9 (2021) 6434–6443, https://doi.org/10.1039/D1BM01074C.

[18] A. Botta, S. Pragliola, V. Venditto, A. Rubino, S. Aprano, A. Del Mauro De, M. G. Girolamo, C.M. Maglione, Synthesis, characterization, and use as emissive layer of white organic light emitting diodes of the highly isotactic poly(N-pentenyl-carbazole), Polym. Compos. 36 (2015) 1110–1117, https://doi.org/10.1002/pc.23445.

[19] A. Botta, V. Venditto, A. Rubino, S. Pragliola, Highly Isotactic Poly(N-butenyl-carbazole): Synthesis, Characterization, and Optical Properties, J. Chem. 2016 (2016) 1656459, https://doi.org/10.1155/2016/1656459.

[20] S. Jeong, I.T. Jung, K.B. Yoon, Intra-/Intermolecular excimer emission of syndiotactic polystyrene having carbazole substituents, Polym.-Korea 35 (2011) 314–319, https://doi.org/10.7317/pk.2011.35.4.314.

[21] A. Botta, S. Pragliola, C. Capacchione, A. Rubino, R. Liguori, A. De Girolamo Del, V. V. Mauro, Synthesis of poly(4-(N-carbazolyl)methyl styrene)s: Tailoring optical properties through stereoregularity, Eur. Polym. J. 88 (2017) 246–256, https://doi.org/10.1016/j.eurpolymj.2017.01.032.

[22] K.S. Roberts, N.S. Sampson, A Facile Synthetic Method to Prepare Fluorescently Labeled ROMP Polymers, Org. Lett. 6 (2004) 3253–3255, https://doi.org/10.1021/ol048935y.

[23] M. Hollauf, G. Trimmel, A.C. Knall, Dye-functionalized polymers via ring opening metathesis polymerization: principal routes and applications, Monatsh. Chem. 146 (2015) 1063–1080, https://doi.org/10.1007/s00706-015-1493-9.

[24] E.K. Riga, D. Boschert, M. Vöhringer, V.T. Widyaya, M. Kurowska, W. Hartleb, K. Lienkamp, Fluorescent Romp monomers and copolymers for biomedical applications, Macromol. Chem. Phys. 218 (2017) 1700273, https://doi.org/10.1002/macp.201700273.

[25] C. Slugovc, The ring opening metathesis polymerisation toolbox, Macromol. Rapid Commun. 25 (2004) 1283–1297, https://doi.org/10.1002/marc.200400150.

[26] C.W. Bielawski, R.H. Grubbs, Living ring-opening metathesis polymerization, Prog. Polym. Sci. 32 (2007) 1–29, https://doi.org/10.1016/j.progpolymsci.2006.08.006.

[27] A. Leitgeb, J. Wappel, C. Slugovc, The ROMP toolbox upgraded, Polymer 51 (2010) 2927–2946, https://doi.org/10.1016/j.polymer.2010.05.002.

[28] T.-L. Choi, R.H. Grubbs, Controlled Living Ring-Opening-Metathesis Polymerization by a Fast-Initiating Ruthenium Catalyst, Angew. Chem. Int. Ed. 42 (2003) 1743–11174, https://doi.org/10.1002/anie.200250632.

[29] S. Sutthasupa, M. Shiotsuki, F. Sanda, Recent advances in ring-opening metathesis polymerization, and application to synthesis of functional materials, Polym. J. 42 (2010) 905–915, https://doi.org/10.1038/pj.2010.94.

[30] Y. Chen, M.M. Abdellatif, K. Nomura, Olefin metathesis polymerization: Some recent developments in the precise polymerizations for synthesis of advanced materials (by ROMP, ADMET), Tetrahedron 74 (6) (2018) 619–643, https://doi.org/10.1016/j.tet.2017.12.041.

[31] M. Buchmeiser, Functional precision polymers via stereo- and regioselective polymerization using group 6 metal alkylidene and group 6 and 8 metal alkylidene *N*-heterocyclic carbene complexes, Macromol. Rapid Commun. 40 (2019) 1800492, https://doi.org/10.1002/marc.201800492.

[32] O.M. Ogba, N.C. Warner, D.J. O'Leary, R.H. Grubbs, Recent advances in ruthenium-based olefin metathesis, Chem. Soc. Rev. 47 (12) (2018) 4510–4544, https://doi.org/10.1039/C8CS00027A.

[33] D. Smith, E.B. Pentzer, S.T. Nguyen, Bioactive and Therapeutic ROMP Polymers, Polym. Rev. 47 (3) (2007) 419–459, https://doi.org/10.1080/15583720701455186.

[34] J.M. Sarapas, C.M. Backlund, B.M. deRonde, L.M. Minter, G.N. Tew, ROMP- and RAFT-based guanidinium-containing polymers as scaffolds for protein mimic synthesis, Chem Eur J 23 (28) (2017) 6858–6863, https://doi.org/10.1002/chem.201700423.

[35] Q. Chen, Surface-Initiated Ring-Opening Metathesis Polymerization (SI-ROMP): History, General Features, and Applications in Surface Engineering with Polymer Brushes, International Journal of Polymer Science (2021), 667704, https://doi.org/10.1155/2021/6677049.

[36] J. Wu, Y. Fu, W. Liu, X. Liao, M. Xie, R. Sun, Synthesis and properties of tricarbazole-functionalized poly(norbornene-dicarboximide), Eur. Polym. J. 76 (2016) 110–121, https://doi.org/10.1016/j.eurpolymj.2016.01.037.

[37] M.P. Thompson, L.M. Randolph, C.R. James, A.N. Davalos, M.E. Hahna, N. C. Gianneschi, Labelling polymers and micellar nanoparticles via initiation, propagation and termination with ROMP, Polym. Chem. 5 (2014) 1954–1964, https://doi.org/10.1039/C3PY01338C.

[38] W. Lang, G. Cheng, R. Peng, Q.-Y. Cao, Rhodamine-anchored poly(norbornene) for fluorescent sensing of ATP, Dyes Pigm. 189 (2021), 109245, https://doi.org/10.1016/j.dyepig.2021.109245.

[39] L.T. Birchall, S. Shehata, S. McCarthy, H.J. Shepherd, E.R. Clark, C.J. Serpell, S.C. G. Biagini, Supramolecular behaviour and fluorescence of rhodamine-functionalised ROMP polymers, Polym. Chem. 11 (2020) 5279–5285, https://doi.org/10.1039/D0PY00799D.

[40] U.R. Gandra, A. Sinopoli, S. Moncho, M. NandaKumar, D.B. Ninković, S.D. Zarić, M. Sohail, S. Al-Meer, E.N. Brothers, N.A. Mazloum, M. Al-Hashimi, H.S. Bazzi, Green Light-Responsive CO-Releasing Polymeric Materials Derived from Ring-Opening Metathesis Polymerization, ACS Appl. Mater. Interfaces 11 (2019) 34376–34384, https://doi.org/10.1021/acsami.9b12628.

[41] P.-S. Yao, Q.-Y. Cao, R.-P. Peng, J.-H. Liu, Quinoline-functionalized norbornene for fluorescence recognition of metal ions, J. Photochem. Photobiol. A Chem. 305 (2015) 11–18. Doi: 10.1016/j.jphotochem.2015.03.003 [.

[42] U.R. Gandra, R. Courjaret, K. Machaca, M. Al-Hashimi, H.S. Bazzi, Multifunctional rhodamine B appended ROMP derived fluorescent probe detects Al3+ and selectively labels lysosomes in live cells, Sci. Rep. 10 (2020) 19519, https://doi.org/10.1038/s41598-020-76525-0.

[43] R.L. Maust, P. Li, B. Shao, S.M. Zeitler, P.B. Sun, H.W. Reid, L.N. Zakharov, M. R. Golder, R. Jasti, Controlled Polymerization of Norbornene Cycloparaphenylenes Expands Carbon Nanomaterials Design Space, ACS Cent. Sci. 7 (2021) 1056–1065, https://doi.org/10.1021/acscentsci.1c00345.

[44] A.M. Polgar, J. Poisson, C.J. Christopherson, Z.M. Hudson, Enhancement of Red Thermally Assisted Fluorescence in Bottlebrush Block Copolymers, Macromolecules 54 (2021) 7880–7889, https://doi.org/10.1021/acs.macromol.1c01524.

[45] S. Shao, J. Hu, X. Wang, L. Wang, X. Jing, F. Wang, Blue thermally activated delayed fluorescence polymers with nonconjugated backbone and through-space charge transfer effect, J. Am. Chem. Soc. 139 (2017) 17739–17742, https://doi.org/10.1021/jacs.7b10257.

[46] C.-T. Lo, Y. Abiko, J. Kosai, Y. Watanabe, K. Nakabayashi, H. Mori, Synthesis and Optoelectronic Properties of Block and Random Copolymers Containing Pendant Carbazole and (Di)phenylanthracene, Polymers 10 (2018) 721, https://doi.org/10.3390/polym10070721.

[47] Q. Li, J. Hu, J. Lv, X. Wang, S. Shao, L. Wang, X. Jing, F. Wang, Through-Space Charge-Transfer Polynorbornenes with Fixed and Controllable Spatial Alignment of Donor and Acceptor for High-Efficiency Blue Thermally Activated Delayed Fluorescence, Angew. Chem. Int. Ed. 59 (2020) 20174–20182, https://doi.org/10.1002/anie.202008912.

[48] X. Zeng, J. Luo, T. Zhou, T. Chen, X. Zhou, K. Wu, Y. Zou, G. Xie, S. Gong, C. Yang, Using ring-opening metathesis polymerization of norbornene to construct thermally activated delayed fluorescence polymers: High-efficiency blue polymer light-emitting diodes, Macromolecules 51 (2018) 1598–1604, https://doi.org/10.1021/acs.macromol.7b02629.

[49] A. de la Escosura, M.V. Martínez-Díaz, T. Torres, R.H. Grubbs, D.M. Guldi, H. Neugebauer, C. Winder, M. Drees, N. Serdar Sariciftci, New donor-acceptor materials based on random polynorbornenes bearing pendant phthalocyanine and fullerene units, Chem. Asian J. 1–2 (2006) 148–154, https://doi.org/10.1002/asia.200600090.

[50] R. Troiano, M. Carratù, S. Pragliola, A.C. Boccia, F. Grisi, ROMP of norbornene and oxanorbornene derivatives with pendant fluorophore carbazole and coumarin groups, Eur. Polym. J. 167 (2022), 111065, https://doi.org/10.1016/j.eurpolymj.2022.111065.

[51] S. Pragliola, A. Botta, R. Troiano, V. Paradiso, F. Grisi, Synthesis and ring-opening metathesis polymerization of a new norbornene dicarboximide with a pendant carbazole moiety, Int. J. Polym. Sci. (2019), https://doi.org/10.1155/2019/5306912.

[52] J.J.V. Grazulevicius, P. Strohriegl, J. Pielichowskic, K. Pielichowskic, Carbazole containing polymers: synthesis, properties and applications, Prog. Polym. Sci. 28 (2003) 1297–1353, https://doi.org/10.1016/S0079-6700(03)00036-4.

[53] F. Bekkar, F. Bettahar, I. Moreno, R. Meghabar, M. Hamadouche, E. Hernáez, J. L. Vilas-Vilela, L. Ruiz-Rubio, Polycarbazole and its derivatives: synthesis and applications. A review of the last 10 years, Polymers 12 (2020) 2227, https://doi.org/10.3390/polym12102227.

[54] I. Cazin, E. Rossegger, G. Guedes de la Cruz, T. Griesser, S. Schlogl, Recent advances in functional polymers containing coumarin chromophores, Polymers 13 (2021) 56, https://doi.org/10.3390/polym13010056.

[55] F. Dumur, Carbazole-based polymers as hosts for solution-processed organic light-emitting diodes: Simplicity, efficacy, Org. Electron. 25 (2015) 345–361, https://doi.org/10.1016/j.orgel.2015.07.007.

[56] P. Ledwon, Recent advances of donor-acceptor type carbazole-based molecules for light emitting applications, Org. Electron. 75 (2019), 105422, https://doi.org/10.1016/j.orgel.2019.105422.

[57] K. Iliopoulos, O. Krupka, D. Gindre, M. Sallé, Reversible two-photon optical data storage in coumarin-based copolymers, J. Am. Chem. Soc. 132 (2010) 14343–14345, https://doi.org/10.1021/ja1047285.

[58] D. Gindre, K. Iliopoulos, O. Krupka, M. Evrard, E. Champigny, M. Sallé, Coumarin-containing polymers for high density non-linear optical data storage, Molecules 21 (2016) 147, https://doi.org/10.3390/molecules21020147.

[59] B. Mailhot-Jensen, S. Robu, A. Rivaton, J.-F. Pilichowski, A. Chirita, E. Chilat, G. Dragalina, Carbazole containing copolymers: Synthesis, characterization, and applications in reversible holographic recording, Int. J. Photoenergy 2010 (2010), 945242, https://doi.org/10.1155/2010/945242.

[60] J. Serin, X. Schultze, A. Adronov, J.M.J. Fréchet, Synthesis and study of the absorption and luminescence properties of polymers containing $Ru(BpyMe2)_3^{2+}$ Chromophores and coumarin laser dyes, Macromolecules 35 (14) (2002) 5396–5404, https://doi.org/10.1021/ma020265t.

[61] J.A. Love, J.P. Morgan, T.M. Trnka, R.H. Grubbs, A practical and highly active ruthenium-based catalyst that effects the cross metathesis of acrylonitrile, Angew. Chem. Int. Ed. 41 (21) (2002) 4035–4037, https://doi.org/10.1002/1521-3773(20021104)41:21<4035::AID-ANIE4035>3.0.CO;2-I.

[62] C. Slugovc, S. Riegler, G. Hayn, R. Saf, F. Stelzer, Highly Defined ABC Triblock Cooligomers and Copolymers Prepared by ROMP Using an N-Heterocyclic-

Carbene-Substituted Ruthenium Benzylidene Initiator, Macromol. Rapid Commun. 24 (7) (2003) 435–439, https://doi.org/10.1002/marc.200390062.
[63] R. Troiano, M. Carratù, S. Pragliola, A.C. Boccia, F. Grisi, Spectroscopic data of norbornene and oxanorbornene dicarboximides functionalized with carbazole and coumarin groups, Data Brief 42 (2022), 111065, https://doi.org/10.1016/j.dib.2022.108202.
[64] Fox equation: $[1/T_g(\text{copolymer}) = (W_A/Tg_A) + (W_B/Tg_B)]$, where W_A and Tg_A are the weight fraction and Tg of monomer A, and W_B and Tg_B are the weight fraction and Tg of monomer B.
[65] Theoretical M_n values were based on the monomer/catalyst feed ratio and assumed quantitative initiation and monomer conversion to polymer.
[66] P.C. Johnson, H.W. Offen, Excimer fluorescence of poly(N-vinylcarbazole), J. Chem. Phys. 55 (1971) 2945–2949, https://doi.org/10.1063/1.1676521.
[67] S. Fatima, A. Mansha, S. Asim, A. Shahzad, Absorption spectra of coumarin and its derivatives, Chem. Pap. 76 (2022) 627–638, https://doi.org/10.1007/s11696-021-01902-6.
[68] D. Bogdal, M. Galica, Novel terpolymers containing carbazole, coumarin and Alq3 complexes, Pure Appl. Chem. 91 (2019) 497–508, https://doi.org/10.1515/pac-2018-1018.
[69] J. Li, A.C. Grimsdale, Carbazole-based polymers for organic photovoltaic devices, Chem. Soc. Rev. 39 (2010) 2399–2410, https://doi.org/10.1039/B915995.
[70] X. Zhao, I. Kurganskii, A. Elmali, J. Zhao, A. Karatay, G. Mazzone, M. Fedin, Electron transfer and intersystem crossing in the coumarin-anthracene electron donor-acceptor dyads, Dyes Pigm. 218 (2023), 111480, https://doi.org/10.1016/j.dyepig.2023.111480.